Single Carrier with Index Modulation for Low Power Terabit Systems

Majed Saad, Faouzi Bader, Jacques Palicot, Ali Chamas Al Ghouwayel, Hussein Hijazi

Single Carrier with Index Modulation for Low Power Terabit Systems

Majed Saad[†], Faouzi Bader[†], Jacques Palicot[†], Ali Chamas Al Ghouwayel[§] and Hussein Hijazi[§]

[†]IETR/CentraleSupélec, Campus de Rennes-Cesson-Sévigné, France
[§]International University of Beirut, Beirut, Lebanon
[†]Email: {majed.saad, faouzi.bader, jacques.palicot}@centralesupelec.fr
[§]{ali.ghouwayel, hussein.hijazi}@biu.edu.lb

***Abstract*—Wireless terabit-per-second (Tb/s) links will become an urgent requirement within the next 10 years. However, current methodology for high data rate wireless communication that keep increasing the M-ary modulation schemes and the order of MIMO spatial multiplexing cannot reach Tb/s with a low power consumption. Thus, a new methodology is required with a large bandwidth in the millimeter-wave (mm-Wave) and sub-Terahertz (sub-THz) bands above 90GHz. In addition, it must be able to provide an extremely high spectral efficiency with a low energy consumption. Note that this consumption can be reduced by using constant-envelope modulations such as continuous phase modulation (CPM). However, the CPM has a very low spectral efficiency that limits the desired data rate. This paper suggests a new methodology to reach 1 Tb/s with a low power consumption by using power efficient single carrier with Index Modulation (IM). Simulation results under various uncorrelated/correlated fading channels show that the systems with power efficient modulations as CPM or QPSK can achieve Tb/s with a good performance. Moreover, the link budget and power estimation prove that the constant and near-constant envelope modulations require less than $1-3$ Watts for 1 Tb/s with 10^{-4} un-coded BER. Finally, this paper shows that conveying most of the information bits using IM to reach an ultra-high data rate is more power efficient than high order MIMO spatial multiplexing with large M-ary QAM as used in LTE.**

***Index Terms*—Beyond 5G, millimeter wave, Terahertz systems, terabit-per-second (Tb/s), power consumption.**

I. Introduction

The wireless data rates have doubled every 18 months over the last three decades. In addition, the wireless data traffic is projected to increase by 1000-fold by the year 2020 [1] and is likely to grow by more than 10 000-fold by the year 2030. Similarly, the required data rates are increasing continuously towards Tb/s.

In addition, the ultra-high data rate wireless communication is an emerging requirements for several scenarios and applications that include transmission distances ranging from the very short (few centimeters or less) to relatively long distances of several kilometers [2]. Some of these use cases such as the Close Proximity P2P applications (Kiosk downloading), Intra-Device Communication, Wireless Fronthaul/Backhaul and Data Centers (described by the IEEE Standards Association of IEEE 802.15 WPAN [2] [3] in the band between 250-325GHz, the IEEE 802.11ad [4], and IEEE 802.15.3e [5] in the 60GHz). Moreover, several researchers tried to reach a high data rate but the maximum achieved, to the best of our knowledge, was below 70Gb/s due to hardware and technology limitation in the D-band [6]. Thus, additional breakthrough technologies are necessary to reach the Beyond 5G throughput requirements.

Dense small-cell deployments, centralized Radio Access Network (RAN), advanced MIMO schemes and new mm-Wave bands are key enablers to achieve the expected increase in spectral efficiency and capacity [7]. For this reason, our research in BRAVE project is focused on the mm-Wave and sub-THz band within the range 90GHz-200GHz where a huge bandwidth can be allocated (up to 50GHz aggregated bandwidth) to reach 1Tb/s (100x peak data rate defined in IMT-2020 for 5G) [8]. Also, other researchers are investigating the feasibility of wireless communication at higher frequencies on the true THz band (0.1-10 THz) where a huge contiguous bandwidth is available [9], [10].

In the last decade, the methodology used to enhance the rate was based on increasing the order of M-ary QAM and the size of antenna array for MIMO spatial multiplexing. However, designing similar systems for Tb/s requires an extremely large signal to noise ratio to ensure good performance. In addition, it suffers from large power consumption by power amplifiers (PAs) due to high peak to average power ratio (PAPR) of larger M-ary QAM.

In order to reach this ultra-high data rate, it is important to develop a new wireless communication methodology that achieve a high spectral efficiency with a given power expenditure. For this reason, our methodology investigates the Single-Carrier (SC) waveform which is enabled by [11]:

- The high power efficiency due to lower PAPR compared to multi-carrier (MC) waveform. MC suffers in nature from high PAPR which leads to intensive energy consumption by the PAs and hence negatively influence out-of-band emissions.
- The availability of frequency-flat channels and especially when the large occupied bandwidth is achieved by aggregation of small channels. Note that the propagation above-90 GHz is often characterized by a dominant path [12], obtained either from LoS situation or antenna beam alignment.

Moreover, we propose to benefit from IM and advanced MIMO schemes to enhance the spectral efficiency of the power efficient SC modulation. Note that IM has attracted tremendous attention and it is explored separately and jointly in the spatial, frequency, and temporal domain in the last decades [13]. In addition, these IM techniques convey additional information bits contained implicitly in the index of the selected element among several possible combinations. As example, the element could be the antenna set as generalized spatial modulation [14] [15], sub-carrier group in MC waveform as OFDM-IM [16], or frequency bands and dispersion matrix in space-time domain as Space-Time-Frequency Shift Keying (STFSK) [17].

In this paper, we propose a new methodology based on constant or near-constant envelope sc modulation with IM (SC-IM) to reach Tb/s with a low power consumption. In addition, its feasibility is evaluated depending on error performance, power consumption, complexity and cost. The performance analysis of the proposed SC-IM is addressed over spatially correlated/uncorrelated Rician and Rayleigh channels. Moreover, the link budget is calculated and the power consumption is estimated to emphasize the importance of SC-IM for Tb/s. Finally, the advantage of SC-IM in mm-Wave and sub-THz bands is presented.

This paper is organized as follows. In Section II, the system model is described, whereas the performance analysis is presented in section III. Section IV illustrates the link budget estimation and discusses the feasibility of SC-IM for ultra high data rates in the mm-Wave and sub-THz bands. Finally, concluding remarks are given in Section V.

The notations adopted are as follows. We use capital bold $\mathbf{X}$ for matrices. $(.)^T$ and $(.)^H$ are used to denote respectively the transpose and the Hermitian transpose of a matrix. $(.)^\dagger$ denotes the pseudo inverse of a matrix. $\mathbf{X}_{m,n}$ denotes a matrix with row index m and column index n. $\mathbf{I}_N$ denotes the $N \times N$ identity matrix. $\otimes$ stands for the Kronecker product. $\binom{n}{k}$ denotes the binomial coefficient. $\mathcal{CN}(\mu, \sigma^2)$ denotes the complex normal distribution of a random variable having mean μ and variance σ^2. $\lfloor . \rfloor$ denotes the floor function. $\|.\|$ stands for the Frobenius norm.

II. System and Channel Models

A. System Model

The proposed system model is based on the Generalized Spatial Modulation (GSM) MIMO system with N_t transmit antennas and N_r receive antennas. In this system, the source binary information sequence b is divided into two streams b_1 and b_2 as shown in Fig. 1. The bit-stream b_1 is mapped by the N_a M-ary Amplitude-Phase Modulators (APM) such as QAM, PSK, CPM, etc. The bit-stream b_2 is encapsulated in the index of the selected Transmit Antenna Set (TAS) at each symbol period, where each TAS is formed of N_a activated transmit antenna (TA) out of N_t.

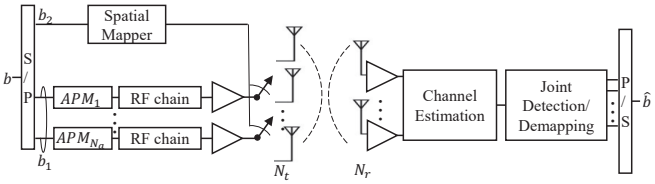

Fig. 1. System Model

The possible number of TAS with N_a activated antennas is the combination $\Omega = \binom{N_t}{N_a}$. However, only $\mathcal{L} = 2^{\lfloor log_2(\Omega) \rfloor}$ are used to keep the bits length of b_2 an integer number and the other possibility are marked as illegal combinations. Note that the appropriate TASs should be carefully selected from the Ω possibilities to minimize the interference and the effect of spatial correlation between antennas. Accordingly, the number of bits per GSM symbol can be expressed as:

$$b = \lfloor log_2(\Omega) \rfloor + N_a . log_2(M) \tag{1}$$

The GSM transmitted symbol vector is $x = [x_1, \ldots, x_{N_t}]^T$ where only the entries corresponding to the active antenna are non-zero. Note that the inter-antenna synchronization at the transmitter is required to make sure that the receiver can detect the activated antenna from each received vector y. The received signal y is expressed as:

$$y = \sqrt{\frac{\rho}{N_a}} \mathbf{H} x + v \tag{2}$$

where $\mathbf{H}$ is the $N_r \times N_t$ channel matrix. ρ is the the average signal to noise ratio (SNR) at each receive antenna, v is $N_r \times 1$ channel noise vector and its elements v_r obeys the independent and identically distributed (i.i.d.) additive white Gaussian noise (AWGN) with the variance of $\sigma_v^2 = 1$, i.e, $\mathcal{CN}(0, 1)$ for $r = 1, \ldots, N_r$.

At the receiver side, the index of selected TAS and the modulated symbols on all activated transmit antennas can be detected jointly by the ML detector that perform exhaustive search over all the possible transmit vector described as

$$\widehat{x} = arg \min_{x \in \chi} \|y - \mathbf{H} x\|^2 \tag{3}$$

where χ denotes the set of all possible transmit vectors in both the spatial and signal constellation domains and $\widehat{x}$ is the estimated transmit vector with N_a non zero elements in the position of the activated transmit antennas.

However, a GSM symbol detection with lower complexity is possible by ordered block minimum mean-squared error (OB-MMSE) that achieves near-ML performance [18]. The OB-MMSE detector reduces the iterations of search algorithm by ordering the appropriate TAS and stop the search when $\|y - \mathbf{H}\widehat{s}\|^2$ becomes less than a predefined threshold $V_{th} = 2N_r\sigma^2$, where $\widehat{s}$ is the MMSE equalized symbol and quantized to an APM symbol. For instance, the sorted TASs are denoted by $\{I_1, I_2, \ldots, I_{\mathcal{L}}\}$ where each I_i represents a vector with the indices of the N_a possible activated TA. Their

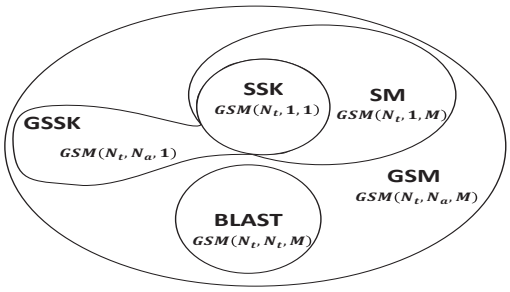

Fig. 2. GSM Derivatives

descending order sorting is based on their weighting factor w_i that measures the reliability of each TAS I_i defined as

$$z_t = (h_t)^{\dagger} y \tag{4}$$

$$w_i = \sum_{n=1}^{N_a} z_{i_n}^2 \tag{5}$$

where $(h_t)^{\dagger} = \frac{h_t^H}{h_t^H h_t}$ is the pseudo inverse of the t^{th} column of channel matrix $\mathbf{H}$ with $t = 1, \ldots, N_t$. Thus z_{i_n} represents the element from $z = [z_1, z_2, \ldots, z_{N_t}]$ at the n^{th} activated TA according to TAS I_i where $i = 1, \ldots, \mathcal{L}$.

Then, the symbol vector is estimated by a simplified block based MMSE equalizer

$$\widehat{s_i} = \mathcal{Q}\left(\left(\left(\mathbf{H}_{I_i}\right)^H \left(\mathbf{H}_{I_i}\right) + \sigma_v^2 \mathbf{I}_{N_a} \right)^{-1} \left(\mathbf{H}_{I_i}\right)^H y \right) \tag{6}$$

where $\mathcal{Q}$ represents the quantization operation that restricts $\widehat{s_i}$ to be a value from the APM constellation set $\mathcal{S}$ and the $N_r \times N_a$ matrix $\mathbf{H}_{I_i}$ is a sub-matrix with all columns of $\mathbf{H}$ corresponding to the antenna indices in TAS I_i. Thus, the reduced computational complexity of OB-MMSE detector can be expressed in terms of real floating point operations according to [18] as following

$$\begin{aligned} Complexity_{OB-MMSE} &= (14N_rN_t + 3N_t + N.N_a)/\mathcal{L} \\ &+ (12N_rN_a^2 + 11N_rN_a + 6N_r - 6N_a^2)p_{avg}/\mathcal{L} \end{aligned} \tag{7}$$

where p_{avg} represents the average number of the block MMSE detections in Eq. (6).

The adopted notation for this system is GSM(N_t, N_a, M) where the parameter M is the APM M-ary size, $M = 2^p$ with $p \geq 0$. Note that $p = 0$ means that the transmitted symbols are just a constant power value to simplify the receiver detection at the expense of lower data rate. Furthermore, it worth mentioning that GSM includes other spatial modulation techniques such as the Spatial Modulation (SM) GSM$(N_t, 1, M)$ [19], Space-Shift Keying (SSK) GSM$(N_t, 1, 1)$ [20], Generalized SSK (GSSK) GSM$(N_t, N_a, 1)$ [21] and conventional MIMO spatial multiplexing defined by Bell Laboratories Layered Space-Time (BLAST scheme) GSM(N_t, N_t, M) as shown in Fig. 2. This feature can be utilized to have a reconfigurable architecture with different data rates and receiver complexity.

B. Channel Model

In this paper, we consider a slow fading MIMO channel matrix $\mathbf{H}$ as a Rayleigh or Rician multipath fading channel with/without spatial correlation defined as

$$\mathbf{H} = \sqrt{\frac{K}{K+1}}\mathbf{H}_{LoS} + \sqrt{\frac{1}{K+1}}\mathbf{\Sigma}_r^{\frac{1}{2}}\mathbf{H}_{NLoS}\mathbf{\Sigma}_t^{\frac{1}{2}T} \tag{8}$$

where K is the Rician factor, $\mathbf{H}_{LoS}$ and $\mathbf{H}_{NLoS}$ are the $N_r \times N_t$ line of sight (LoS) and the non-LoS channel matrix respectively. The $\mathbf{H}_{NLoS}$ can be considered as a Rayleigh channel whose elements satisfies $\mathcal{CN}(0, 1)$. In addition, the NLoS part exhibits a spatial correlation described by Kronecker model that assumes the spatial correlations at the transmit and receive sides are separable. This model approximates the correlation matrix $\mathbf{\Sigma}$ as the Kronecker product of the correlation matrices at transmitter and receiver, denoted as $\mathbf{\Sigma}_t$, and $\mathbf{\Sigma}_r$, respectively:

$$\mathbf{\Sigma} = \mathbf{\Sigma}_t \otimes \mathbf{\Sigma}_r \tag{9}$$

Thus, Eq. (8) includes the uncorrelated/correlated Rayleigh and Rician fading channel as special case depending on the value of K and the correlation matrices.

III. Performance Analysis

In this section, firstly we compare MIMO spatial multiplexing (BLAST) with GSM to prove that the latter is able to reduce the number of required RF chains as depicted in Fig. 3 for a given system spectral efficiency. The target system spectral efficiency in Fig. 3 is in the order of 25 b/s/Hz for $N_t \leq 32$. It is clear that the number of RF chains with BLAST is always the largest and it is more than the double of that of GSM when the APM spectral efficiency is low (up to 3b/s/Hz). This reduction leads to a lower detector complexity for GSM compared to BLAST. However, these advantages of GSM are at the price of higher number of transmit antennas which is feasible for example for downlink scenario as Kiosk downloading at mm-Wave and sub-THz bands.

In the following, we present the numerical comparison between several APM-GSM systems that employs different APM schemes:PSK, DPSK, CPM and QAM. The bit error rate (BER) of these systems in function of the average SNR was evaluated using Monte Carlo Simulations. In order to conduct a fair comparison, same transmission rate has been used without restriction on the constellation size and the number of antennas.

In fact, the GSM(N_t, N_a, M) parameters for Tb/s are chosen such that the required number of RF chains is minimized to reduce the cost with a maximum allowed $N_t \leq 22$ and a given M-ary APM. In addition, the adopted GSM detector in these systems is OB-MMSE that is able to jointly detect the TAS and the APM constellations with a balanced trade-off between system performance and complexity. The simulations are performed over correlated/uncorrelated Rayleigh and Rician channels with different correlation levels. The correlation matrices in the Kronecker model are formed according to the exponential model of [22] where the elements of transmit

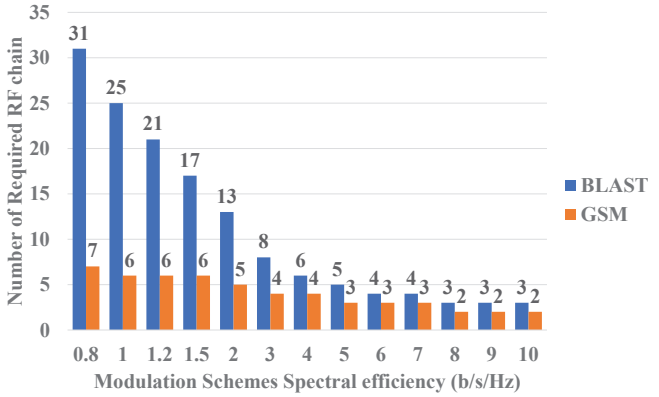

Fig. 3. Minimum number of required RF chains for GSM and BLAST systems as function of APM spectral efficiency. System Spectral efficiency is in the order of 25 b/s/Hz.

$\mathbf{\Sigma}_t$ and receive $\mathbf{\Sigma}_r$ correlation matrices are affected by fixed correlation factor β: $[\mathbf{\Sigma}_t]_{m,n} = \beta_t^{|m-n|}$. We used $\mathbf{\Sigma}_r = I_{N_r}$ to concentrate on the impact of correlation at the transmitter side where a larger antenna array is used to convey the data in the spatial domain of index modulation.

The simulation parameters for the different systems that can achieve Tb/s are summarized in Table I. The CPM parameters used with CPM-GSM system are: modulation index $h = \frac{1}{3}$, raised cosine as frequency pulse with length $L = 3$ symbol intervals.

TABLE I
SIMULATION PARAMETERS

Parameters	Value
CPM-GSM	GSM$(22, 6, 4)$
QPSK-GSM	GSM$(17, 6, 4)$
DQPSK-GSM	GSM$(17, 6, 4)$
16QAM-GSM	GSM$(13, 4, 16)$
64QAM-GSM	GSM$(11, 3, 64)$
256QAM-GSM	GSM$(24, 2, 256)$
N_r	$2N_a$
Rician factor K	$[0,\ 3]$
Oversampling factor	2
Raised Cosine Rolloff α	0.2
Correlation factor β_t	$[0,\ 0.2,\ 0.5,\ 0.8]$
Number of GSM symbols	10^4

Fig. 4 shows the performance of differents systems over uncorrelated Rayleigh channel. As we remark, systems with more data conveyed by IM with small M-ary size as (D)QPSK-GSM and CPM-GSM have better performance than those with a lower number of antennas but with higher M-ary size $M \geq 16$. Therefore, the total BER is affected by the order of APM being used more than the order of index modulation. In other words, the larger N_t and lower M-ary APM are, the better the performance is. But increasing N_t increases the computational complexity of the detector.

The same systems are evaluated over uncorrelated Rician channel and the simulation results are shown in Fig. 5. However, the required SNR in this channel is higher than that in Rayleigh channel for same BER. It is worth mentioning

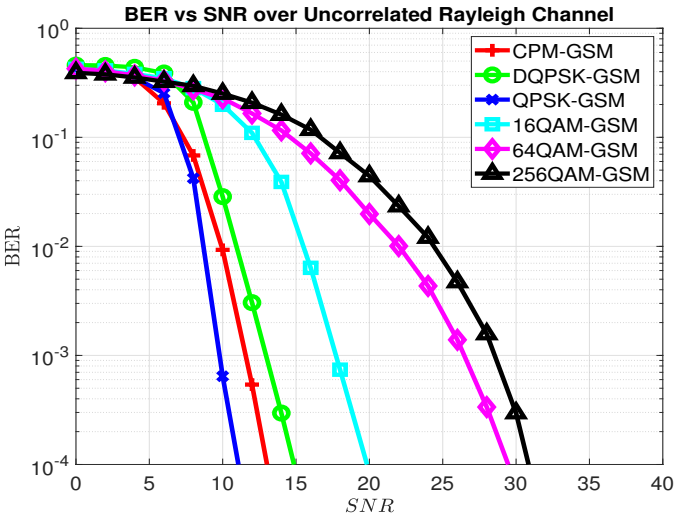

Fig. 4. BER vs SNR for various systems over uncorrelated Rayleigh channel

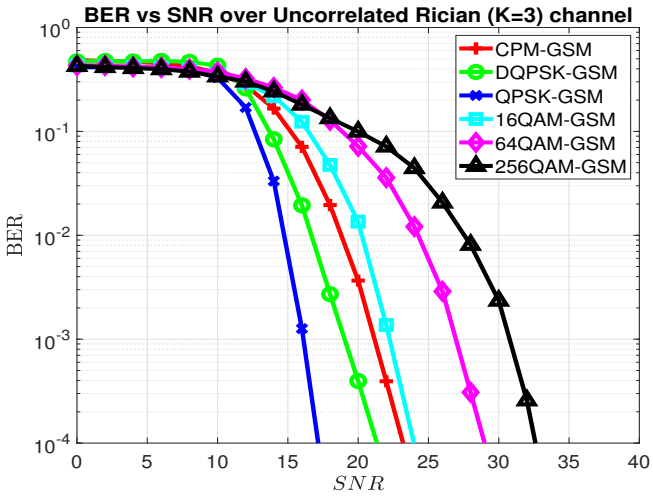

Fig. 5. BER vs SNR for various systems over uncorrelated Ricain channel

that CPM-GSM have a notable degradation in the Rician channel about $10dB$ and this system requires additional $2dB$ compared to DQPSK-GSM while it was completely the inverse in Rayleigh channel.

CPM-GSM and (D)QPSK-GSM are compared in Fig. 6 and 7 with different correlation levels $\beta_t = [0.2,\ 0.5,\ 0.8]$ over Rayleigh and Rician channels respectively. These results show that these systems conserve their good performance with low spatial correlation while they start to degrade at high correlation levels. In particular, (D)QPSK-GSM performance is reduced by less than $1dB$ at un-coded BER$= 10^{-4}$ when the correlation increases to $\beta_t = 0.5$ as shown in Fig. 6 and 7. Also, their performance degrades by approximately $5dB$ at high correlation level $\beta_t = 0.8$, while CPM-GSM is more sensitive to correlation and degrades by $6 - 8dB$.

Furthermore, the spatial correlation that is larger at high frequencies with uniform planar array [23] affects the performance of any spatial modulation with multiple active transmit

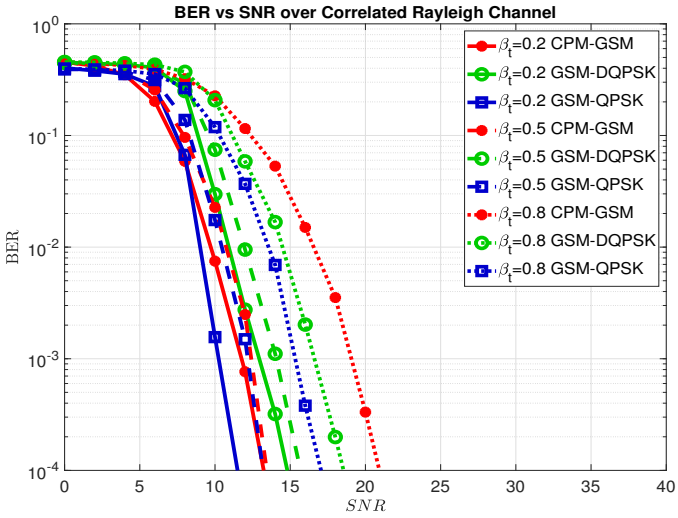

Fig. 6. BER vs SNR for (D)QPSK-GSM and CPM-GSM over correlated Rayleigh channel

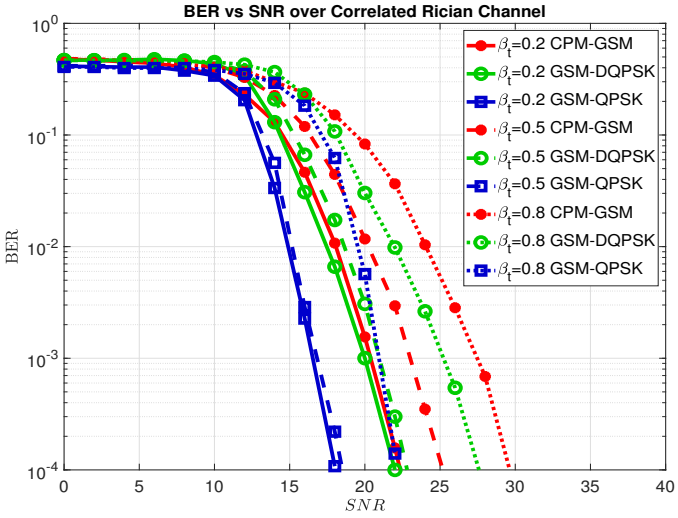

Fig. 7. BER vs SNR for (D)QPSK-GSM and CPM-GSM over correlated Rician channel

antennas. However, its effect can be reduced by carefully choosing the appropriate TAS and their elements.

In reality, a perfect channel estimation can not be guaranteed and the results in [24] show that the channel estimation error degrades rapidly the performance of large M-ary QAM ($M = 16$) and creates an error floor at BER= 10^{-5} or higher while its effect on low M-ary as QPSK is less important and the error floor is as low as BER= 10^{-7}. Thus, these low M-ary APM which have near-constant or constant envelope are more robust to channel estimation errors.

IV. Link Budget and Discussion

In this section, the link budget is calculated for all systems for same un-coded BER 10^{-4} with correlated/uncorrelated Rayleigh and Rician channels. Then, their power consumption for an ultra-high data rate is deduced. For a fair comparison, these systems are configured for same spectral efficiency that is defined as:

$$SE_{GSM} = \frac{BitRate_{(bits/s)}}{W_{(Hz)}} = \frac{R_{(Symbol/s)} * b_{(bits/symbol)}}{W(Hz)} \tag{10}$$

where R is the symbol rate and W is the allocated bandwidth. Since the non-linear modulation as CPM requires a larger bandwidth, its symbol rate is adjusted accordingly to keep the same occupied bandwidth among all systems. Thus, the number of bits per GSM symbol must be higher with CPM as shown in Table II.

Henceforth, we consider a close proximity scenarios (as Downlink kiosk) with distance d=5m and channel bandwidth W=1GHz with channel aggregation/bounding. Note that the available spectrum is 49.65GHz in the frequency range between 92GHz and 175GHz according to [8] and 50GHz contiguous spectrum between 275-325GHz [2].

Note that the receivers in this scenario are low cost mobile devices that have small antenna gain. However, this gain is higher when considering longer distances with other scenario as Wireless Backhaul.

In Table II, the required transmit power P_t with small distance communication is calculated from the required SNR according to the following parameters:

$N_{Thermal}$	$= 10log_{10}(k.T.W) + 30$	dBm
N_{Floor}	$= N_{Figure} + N_{Thermal}$	dBm
Rx_{Level}	$= SNR + N_{Floor}$	dBm
$fspl$	$= 20log_{10}(\frac{4\pi df_c}{c})$	dB
$T_{PathLoss}$	$= fspl + Attenuation$	dB
$EIRP$	$= T_{PathLoss} - G_r + L_{crx} + Rx_{Level}$	dBm
P_t	$= EIRP - G_t + L_{ctx}$	dBm

where k, T, N_{Figure}, $fspl$, f_c, C, G_r/G_t, L_{crx}/L_{ctx} and $EIRP$ are Boltzmann constant, the temperature in kelvin, the noise figure, the free space path loss, the carrier frequency, the speed of light in vacuum ($c = 3 \times 10^8 m/s$), receive/transmit antenna gain, receiver/transmitter cable loss, the effective isotropic radiated power respectively.

Furthermore, the power consumption is deduced based on the power amplifier efficiency which is affected by the APM PAPR. Consequently, the constant and near-constant envelope modulations combined with GSM prove their ability to reach a high throughput of 1 Tb/s. Also, they conserve their low power consumption as shown in Table II that is limited to few Watts while large M-ary APM-GSM requires more $15 - 20dB$. In addition, it is worth mentioning that CPM-GSM have the lowest power consumption in Rayleigh channel but this behavior changes with the spatial correlation effect or in Rician channel due to its performance degradation. Therefore, QPSK-GSM system becomes the least power consuming system. Whereas the DPQSK-GSM system requires more power compared to CPM-GSM and QPSK-GSM, but it is more robust to phase noise that is an important impairment in the sub-THz bands.

The high M-ary APM-GSM systems exceeds the maximum allowed EIRP limitations $40dBm$, even the 16QAM requires $11dBm$ as transmit power which is greater than the actual

TABLE II
LINK BUDGET AND POWER CONSUMPTION FOR DIFFERENT GSM PARAMETERS ACHIEVING Tb/s

Parameters	Temperature (degree C)	20	Carrier Frequency (GHz)		150	Distance (m)		5
	99% of Channel Bandwidth (GHz)	1	Number of Channel Aggregation/bounding		44	Total Bandwidth (GHz) [8]		44
	Modulation	**CPM**	**π/4-QPSK**	**π/4-DQPSK**	**16-QAM**	**64-QAM**	**256-QAM**	**Units**
	GSM (Nt,Na)	(22,6)	(17,6)	(17,6)	(13,6)	(11,3)	(4,3)	
	Bits per GSM symbol	28.00	25.00	25.00	25.00	25.00	26.00	bits
	Symbol Rate (R)	0.80	0.92	0.91	0.91	0.92	0.91	GSym/s
Rate	APM Spectral Efficiency	1.59	1.83	1.82	3.65	5.49	7.3	bps/Hz
	GSM Spectral Efficiency	22.26	22.90	22.80	22.83	22.88	23.71	bps/Hz
	Total Throughput	**979.4**	**1007.6**	**1003.2**	**1004.3**	**1006.5**	**1043.328**	**Gbps**
Receiver	**SNR with Rayleigh**	13.00	12.00	15.00	20.00	29.00	31.00	dB
	RX Noise Figure (NF)	10.00						dB
	Thermal Noise (Nthermal)	-83.93						dBm
	Noise floor	**-73.93**						**dBm**
	Rx Signal Level	**-60.93**	**-61.93**	**-58.93**	**-53.93**	**-44.93**	**-42.93**	**dBm**
	RX Cable Loss (Lcrx)	1						dB
	RX Antenna Gain (Gr)	3						dBi
Channel	Free space path loss (fspl)	89.94						dB
	Vapour attenuation	1.28						dB/Km
	O2 attenuation	0.01						dB/Km
	Rain attenuaton	11.78						dB/Km
	Total Path loss	**90.01**						**dB**
Transmitter	Required Tx EIRP	27.08	26.08	29.08	34.08	**43.08**	**45.08**	dBm
	Cable Loss (Lctx)	1						dB
	TX Antenna Gain (Gt)	24						dBi
	Required Pt	**4.08**	**3.08**	**6.08**	**11.08**	**20.08**	**22.08**	**dBm**
PAPR	PAPR for (α=0.2)	0	3.8	4.86	7.5	8.2	8.35	dB
	Theoratical PA Efficiency	0.8	0.52	0.44	0.34	0.3	0.28	
Uncorrelated	**Power per Channel**	**3.20**	**3.91**	**9.21**	**37.70**	**339.40**	**576.34**	**mW**
	Total Power Consumption	**0.14**	**0.17**	**0.41**	**1.66**	**14.93**	**25.36**	**W**
		21.48	**22.35**	**26.08**	**32.20**	**41.74**	**44.04**	**dBm**
	SNR with Rician K=3	23.00	17.00	21.00	24.00	29.00	31.00	dB
	Total Power Consumption	31.48	27.35	32.08	36.20	41.74	44.04	dBm
Correlated	**SNR with Rayleigh β=0.8**	21.00	17.00	18.00				dB
	Total Power Consumption	29.48	27.35	29.08				dBm
	SNR with Rician β=0.8	29.00	22.00	27.00				dB
	Total Power Consumption	37.48	32.35	38.08				dBm

transmit power ($P_t < 10dBm$) at the THz frequencies with current technologies.

Moreover, a high M-ary schemes also require a power-hungry analog to digital and digital to analog converters (ADC/DAC) with a large resolution. While the low order modulation schemes allow the usage of few bits ($1-3$ bits ADC) that is a critical requirements to allow higher speed ADC for a larger bandwidth with a low cost. Therefore, the high M-ary APM-GSM systems are not suitable for high data rate in the order of Tb/s with power constraint.

However, the advantages of the CPM-GSM and (D)QPSK-GSM systems come with an increase of the detector complexity and the number of transmit antennas compared to high order modulation with GSM. Note that these computational complexities and the required number of antennas with GSM are less than those with MIMO spatial multiplexing (BLAST) combined with same APM for similar system spectral efficiency. Another advantage of QPSK system is the ability to perform the demodulation in the analog domain that reduces the required converters resolution [25], where they implement a multi-Gb/s analog synchronous QPSK demodulator with phase-noise suppression.

Finally, any system requires a higher SNR in a more severe channels but the analog or hybrid beam-forming gain can keep the systems shown in Fig. 8 feasible in terms of energy

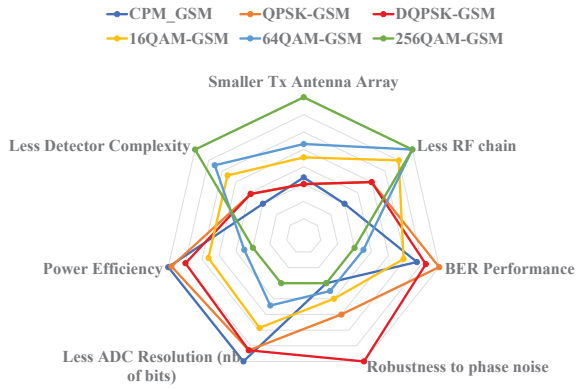

Fig. 8. System comparison between different SC modulations with GSM for achieving a Tb/s (see Table II)

consumption. This feature is enabled by massive MIMO where the number of transmit antennas can be increased by replacing each antenna element in TAS by a small antenna array that performs analog beam-forming as proposed in [26] without increasing the number of RF chains at transmitter nor at the receiver side. Therefore, these constant and near-constant envelope with beamforming aided GSM are very appealing for an ultra-high data rates especially for a Tb/s downlink Kiosk sceanrio, where the power consumption and cost of the receiver of the mobile devices are the most critical constraints.

In brief, the comparison of these APM-GSM systems from different point of view is illustrated in Fig. 8 and it shows that the power efficient (D)QPSK-GSM systems are a balanced trade-off between system performance/power efficiency and hardware cost/detector computational complexity.

V. CONCLUSION

The current methodology for high data rate wireless communication as used in LTE is based on increasing the MIMO spatial multiplexing order and M-ary schemes, but it requires a great effort to reduce the PAPR for limiting the power consumption. This methodology is not a convenient solution for ultra high data rate in the order of Tb/s in the 90GHz-200GHz band especially for low cost implementation where the efficiency and the achievable output power decreases at higher frequencies. Thus, this paper proposes a novel methodology to reach the ultra-high data rates in the order of Tb/s with low power consumption. It is based on using power efficient modulation like constant or near-constant envelope modulation (CPM and (D)QPSK) with GSM or any index modulation that can increase the system spectral efficiency and conserve the power efficiency. The results show that QPSK-GSM(17,6,4) requires 19 dB less than 256QAM-GSM(4,3,256) for same spectral efficiency in Rayleigh channel. Therefore, conveying more data by index modulation have a better performance than reducing the number of antennas and increasing the constellation size to attain same system spectral efficiency. Moreover, the link budget and power consumption is estimated for short distance communication e.g. Downlink Kiosk with

Tb/s data rate and a $44GHz$ bandwidth (available at 90GHz-175GHz band [8]). These estimations prove that with the proposed methodology for Tb/s throughput, less than 1 Watt (21-26 dBm) is sufficient for (D)QPSK-GSM and CPM-GSM in Rayleigh channel and few Watts (32-38 dBm) are more than enough even in highly correlated Rician channel ($\beta_t = 0.8$). Note that QPSK-GSM have the lowest power consumption (27-32 dBm) in highly correlated channel due to its better performance while DQPSK-GSM consumes slightly more power and provides a robustness to phase noise which is an important impairments at sub-THz bands. In conclusion, the proposed methodology proves that the constant or near-constant envelope modulation CPM-GSM and (D)QPSK-GSM systems with limited number of RF chains, feasible antenna array size and acceptable complexity are able to reach a high system spectral efficiency $\approx$ 25b/s/Hz and hence ultra-high data rates while maintaining a low power consumption. Furthermore, this methodology allows the usage of low resolution ADC with low power and cost as required for sub-THz communication. Finally, this paper prove the feasibility of the proposed methodology from different point of view as performance, spectral/power efficiency, complexity and cost. Future work will consider other forms of index modulation and will investigate the receiver fundamental functions at sub-THz such as synchronization and equalization.

ACKNOWLEDGMENT

The research leading to these results received funding from the French National Research Agency (ANR-17-CE25-0013) within the frame of the project BRAVE.

REFERENCES

[1] A. Ghosh et al., "Millimeter-wave enhanced local area systems: A high-data-rate approach for future wireless networks," IEEE Journal on Selected Areas in Communications, vol. 32, no. 6, June 2014.

[2] IEEE 802.15.3d Standard Association, "IEEE 802.15.3d TG3d Applications Requirements Document (ARD)", May-2015.

[3] IEEE 802.15.3d Standard Association, "IEEE Standard for High Data Rate Wireless Multi-Media Networks, Amendment 2: 100 Gb/s Wireless Switched Point-to-Point Physical Layer," 2017.

[4] IEEE 802.11ad Standard Association, "Amendment 3: Enhancements for Very High Throughput in the 60 GHz Band," 2012.

[5] IEEE 802.15.3e Standard Association, "IEEE Standard for High Data Rate Wireless Multi-Media Networks, Amendment 1: High-Rate Close Proximity Point-to-Point Communications," 2017.

[6] I. Ando, M. Tanio, M. Ito, T. Kuwabara, T. Marumoto, and K. Kunihiro, "Wireless D-band communication up to 60 Gbit/s with 64QAM using GaAs HEMT technology," 2016 IEEE Radio and Wireless Symposium (RWS), 2016.

[7] H. J. Song and T. Nagatsuma, "Present and future of terahertz communications," IEEE Transactions on Terahertz Science and Technology, ,Vol. 1, Issue 1, pp.256-263, 2011.

[8] J.-B. Dore, Y. Corre, S. Bicais, J. Palicot, E. Faussurier, D. Ktenas, and F. Bader, "Above-90GHz Spectrum and Single-Carrier Waveform as Enablers for Efficient Tbit/s Wireless Communications," 25th International Conference on Telecommunications (ICT), 2018.

[9] I. F. Akyildiz, J. M. Jornet and C. Han, "Terahertz Band: Next Frontier for Wireless Communications," Physical Communication (Elsevier) Journal, vol. 12, pp. 16-32, September 2014.

[10] I. F. Akyildiz, J. M. Jornet and C. Han, "TeraNets: Ultra-broadband Communication Networks in the Terahertz Band," IEEE Wireless Communications Magazine, vol. 21, no. 4, pp. 130-135, August 2014.

[11] Jacques Palicot and Faouzi Bader, "Backing to Single Carrier in Tera Hertz Communications for Green Considerations", in Proc. of the 32nd International Union of Radio Science (URSI2017) GASS. Montréal, Canada, August 2017.

[12] L. Pometcu, R. Derrico, "Characterization of Sub-THz and mmWave Propagation Channel for Indoor Scenarios," in the Proc. of the 12th European Association on Antennas and Propagation (EurAAP18), April 2018.

[13] N. Ishikawa, S. Sugiura, and L. Hanzo, "50 Years of Permutation, Spatial and Index Modulation: From Classic RF to Visible Light Communications and Data Storage," IEEE Communications Surveys and Tutorials, vol. 20, no. 3, pp. 19051938, 2018.

[14] A. Younis, N. Serafimovski, R. Mesleh, and H. Haas, "Generalised spatial modulation," in Proc. Signals, Syst. Comput., pp. 1498 1502, 2010.

[15] J. T. Wang, S. Y. Jia, J. Song, "Generalised spatial modulation system with multiple active transmit antennas and low complexity detection scheme," IEEE Trans. Wireless Commun., vol.11, no. 4, pp. 1605-1615, Apr. 2012.

[16] E. Basar, U. Aygolu, E. Panayirci, and H. V. Poor, "Orthogonal Frequency Division Multiplexing With Index Modulation," IEEE Transactions on Signal Processing, vol. 61, no. 22, pp. 55365549, 2013.

[17] H. A. Ngo, C. Xu, S. Sugiura, and L. Hanzo, "Space-Time-Frequency Shift Keying for Dispersive Channels," IEEE Signal Processing Letters, vol. 18, no. 3, pp. 177180, 2011.

[18] Y. Xiao, Z. Yang, L. Dan, P. Yang, L. Yin, and W. Xiang, "Low-Complexity Signal Detection for Generalized Spatial Modulation," IEEE Communications Letters, vol. 18, no. 3, pp. 403-406, 2014.

[19] R. Mesleh, H. Haas, S. Sinaovic, C. W. Ahn, and S. Yun, "Spatial modulation," IEEE Trans. Veh. Technol., vol. 57, no. 4, pp. 2228-2241, July 2008.

[20] Y. A. Chau and S.-H. Yu, "Space modulation on wireless fading channels," IEEE 54th Vehicular Technology Conference (VTC-Fall), Atlantic City, NJ, USA, Oct. 7-11, 2001.

[21] J. Jeganathan, A. Ghrayeb, and L. Szczecinski, "Generalized space shift keying modulation for MIMO channels," IEEE 19th International Symposium on Personal, Indoor and Mobile Radio Communications (PIMRC), 2008.

[22] S. L. Loyka, "Channel capacity of MIMO architecture using the exponential correlation matrix," IEEE Commun. Lett., vol. 5, pp. 369-371, Sept. 2001.

[23] A. Chatterjee, S. Chatterjee, and S. S. Das, "Evaluation of spatial correlation and its effect on channel capacity of uniform planar antenna array," 23rd National Conference on Communications (NCC), 2017.

[24] M. Koca and H. Sari, "Generalized spatial modulation over correlated fading channels: Performance analysis and optimization," IEEE International Conference on Telecommunications (ICT), 2013

[25] A. Ulusoy and H. Schumacher, "Multi-Gb/s Analog Synchronous QPSK Demodulator With Phase-Noise Suppression", IEEE Transactions on Microwave Theory and Techniques, vol. 60, no. 11, pp. 3591-3598, 2012.

[26] N. Ishikawa, R. Rajashekar, S. Sugiura and L. Hanzo, "Generalized Spatial Modulation Based Reduced-RF-Chain Millimeter-Wave Communications", IEEE Transactions on Vehicular Technology, pp. 1-1, 2016.